Communications in Statistics—Simulation and Computation®, 38: 2134–2151, 2009

ISSN: 0361-0918 print/1532-4141 online
DOI: 10.1080/03610910903249536

Simulation of Spatially Correlated Clutter Fields

OSCAR H. BUSTOS[1], ANA GEORGINA FLESIA[1], ALEJANDRO C. FRERY[2], AND M. MAGDALENA LUCINI[3]

[1]Facultad de Matemática Astronomía y Física & CIEM-Conicet, Universidad Nacional de Córdoba, Córdoba, Argentina
[2]Universidade Federal de Alagoas, Instituto de Computação, CPMAT & LCCV, Maceió, Brazil
[3]Facultad de Ciencias Exactas, Naturales y Agrimensura, Universidad Nacional de Nordeste & Conicet, Corrientes, Argentina

Correlated $\mathcal{G}$ distributions can be used to describe the clutter seen in images obtained with coherent illumination, as is the case of B-scan ultrasound, laser, sonar, and synthetic aperture radar (SAR) imagery. These distributions are derived using the square root of the generalized inverse Gaussian distribution for the amplitude backscatter within the multiplicative model. A two-parameter particular case of the amplitude $\mathcal{G}$ distribution, called $\mathcal{G}_A^0$, constitutes a modeling improvement with respect to the widespread $\mathcal{K}_A$ distribution when fitting urban, forested, and deforested areas in remote sensing data. This article deals with the modeling and the simulation of correlated $\mathcal{G}_A^0$-distributed random fields. It is accomplished by means of the Inverse Transform method, applied to Gaussian random fields with spatial correlation. The main feature of this approach is its generality, since it allows the introduction of negative correlation values in the resulting process, necessary for the proper explanation of the shadowing effect in many SAR images.

Keywords Image modeling; Simulation; Spatial correlation; Speckle.

Mathematics Subject Classification 62; 62M40.

1. Introduction

The demand for exhaustive clutter measurements in all scenarios would be alleviated if plausible data could be obtained by computer simulation. Clutter simulation is an important element in the development of target detection algorithms for radar, sonar, ultrasound and laser imaging systems. Using simulated data, the accuracy of clutter models may be assessed and the performance of target detection algorithms

Received June 3, 2009; Accepted August 10, 2009
Address correspondence to Ana Georgina Flesia, CIEM-Conicet and FaMAF-UNC, Medina Allende s/n. Ciudad Universitaria, Córdoba 5000, Argentina; E-mail: gflesia@gmail.com

may be quantified against controlled clutter backgrounds. This article is concerned with the simulation of random clutter having appropriate both first and second order statistical properties.

The use of correlation in clutter models is significant and relevant since correlation effects often dominate system performance. Models merely based on single-point statistics could, therefore, produce misleading results, and several commonly used forms for clutter statistics fall into this category.

The statistical properties of heterogeneous clutter returned by Synthetic Aperture Radar (SAR) sensors have been largely investigated in the literature. A theoretical model widely adopted for these images assumes that the value in every pixel is the observation of an uncorrelated stochastic process Z_A, characterized by its single-point (first-order) statistics. A general agreement has been reached that the amplitude fields are well explained by the $\mathcal{K}_A$ distribution. Such distribution arises when coherent radiation is scattered by a surface having gamma-distributed cross-section fluctuations. Although agricultural fields and forest on flat areas are very well fitted by this distribution, it is also known that it fails giving accurate statistical descriptions of extremely heterogeneous data, such as urban areas and forest growing on undulated relief.

As discussed in Frery et al. (1997, 1999), another distribution, the $\mathcal{G}_A$ law, can be used to describe those extremely heterogeneous regions, with the advantage that it has the $\mathcal{K}_A$ distribution as a particular case. This distribution arises in coherent imaging applications as a result of the action of multiplicative speckle noise on an underlying square root of a generalized inverse Gaussian distribution. The main drawback of this general model is that it requires an extra parameter, besides its theoretical complexity.

Nevertheless, it can be seen in Frery et al. (1997) and Mejail et al. (2000) that another special case of the $\mathcal{G}_A$ distribution, namely the $\mathcal{G}_A^0(\alpha, \gamma, n)$ law, which has as many parameters as the $\mathcal{K}_A$ distribution, is able to model with accuracy extremely heterogeneous clutter. The number of looks, n, is fixed for the whole image and describes the signal-to-noise overall ratio. Relevant information can be extracted by estimating α and γ as, for instance, thematic maps (see Gambini et al., 2006; Mejail et al., 2003) and maximum a posteriori filters (Moschetti et al., 2006). Frery et al. (2004) provided a technique for dealing with small samples when maximum likelihood estimates are sought. Recent research has focused on improved estimation through data resampling (see Cribari-Neto et al., 2002) and via analytical corrections (see Silva et al., 2008; Vasconcellos et al., 2005, for details). Robust estimators have also been proposed for the parameter estimation of speckled data, c.f. Bustos et al. (2002) and Allende et al. (2006).

More recently, hypothesis tests based on stochastic distances have been proposed for this kind of data (Nascimento et al., in press).

As a consequence, efforts have been directed towards the simulation of $\mathcal{G}_A^0$ textures, but no exact method for generating patterns with arbitrary assigned spatial autocorrelation function and $\mathcal{G}_A^0$ distribution has been envisaged so far. This article tackles the problem of simulating correlated $\mathcal{G}_A^0$ fields.

2. Correlated $\mathcal{G}_A^0$ Clutter

The main properties and definitions of the $\mathcal{G}_A^0$ clutter are presented in this section, starting with the first order properties of the distribution and concluding with the definition of a $\mathcal{G}_A^0$ stochastic process that will describe Z_A fields.

2.1. *Marginal Properties*

The $\mathcal{G}_A^0(\alpha, \gamma, n)$ distribution is characterized by the following probability density function:

$$f_{Z_A}(z, (\alpha, \gamma, n)) = \frac{2n^n\Gamma(n-\alpha)}{\sqrt{\gamma}\Gamma(-\alpha)\Gamma(n)} \cdot \frac{\left(\frac{z}{\sqrt{\gamma}}\right)^{2n-1}}{\left(1+\frac{z^2}{\gamma}n\right)^{n-\alpha}} \cdot \mathbb{I}_{(0,+\infty)}(z), \quad \alpha < 0, \ \gamma > 0, \qquad (1)$$

being $n \geq 1$ the number of looks of the image, which is controlled at the image generation process, and $\mathbb{I}_T(\cdot)$ the indicator function of the set T. The parameter α describes the roughness, being small values (say $\alpha \leq -15$) usually associated to homogeneous targets, like pasture, values ranging in the $(-15, -5]$ interval usually observed in heterogeneous clutter, like forests, and large values ($-5 < \alpha < 0$, for instance) commonly seen when extremely heterogeneous areas are imaged. The parameter γ is related to the scale, in the sense that if Z is $\mathcal{G}_A^0(\alpha, 1, n)$ distributed then $Z_A = \sqrt{\gamma}Z$ obeys a $\mathcal{G}_A^0(\alpha, \gamma, n)$ law.

A SAR image over a suburban area of Munchen, Germany, is shown in Fig. 1. It was obtained with E-SAR, an experimental polarimetric airborne sensor operated by the German Aerospace Agency (Deutsches Zentrum fur Luft-und Raumfahrt DLR). The data here shown were generated in single look format, and exhibit the three discussed types of roughness: homogeneous (the dark areas to the middle

Figure 1. E-SAR image showing three types of texture.

of the image), heterogeneous (the clear area to the left) and extremely heterogeneous (the clear area to the right).

The rth moments of the $\mathcal{G}_A^0(\alpha, \gamma, n)$ distribution are:

$$E(Z_A^r) = \left(\frac{\gamma}{n}\right)^{\frac{r}{2}} \frac{\Gamma(-\alpha - \frac{r}{2})\Gamma(n + \frac{r}{2})}{\Gamma(-\alpha)\Gamma(n)}, \quad \alpha < -r/2, \ \ n \geq 1, \tag{2}$$

when $-r/2 \leq \alpha < 0$ the rth order moment is infinite. Using Eq. (2), the mean and variance of a $\mathcal{G}_A^0(\alpha, \gamma, n)$ distributed random variable can be computed:

$$\mu_{Z_A} = \sqrt{\frac{\gamma}{n}} \frac{\Gamma(n + \frac{1}{2})\Gamma(-\alpha - \frac{1}{2})}{\Gamma(n)\Gamma(-\alpha)},$$

$$\sigma^2_{Z_A} = \frac{\gamma[n\Gamma^2(n)(-\alpha - 1)\Gamma^2(-\alpha - 1) - \Gamma^2(n + \frac{1}{2})\Gamma^2(-\alpha - \frac{1}{2})]}{n\Gamma^2(n)\Gamma^2(-\alpha)}.$$

Figure 2 shows three densities of the $\mathcal{G}_A^0(\alpha, \gamma, n)$ distribution for the single look ($n = 1$) case. These densities are normalized so that the expected value is 1 for every value of the roughness parameter. This is obtained using Eq. (2) for setting the scale parameter $\gamma = \gamma_{\alpha,n} = n(\Gamma(-\alpha)\Gamma(n)/(\Gamma(-a - 1/2)\Gamma(n + 1/2)))^2$. These densities illustrate the three typical situations described above: homogeneous areas ($\alpha = -15$, dashes), heterogeneous clutter ($\alpha = -5$, dots) and an extremely heterogeneous target ($\alpha = -1.5$, solid line).

Following Barndorff-Nielsen and Blæsild (1981), it is interesting to see these densities as log probability functions, particularly because the $\mathcal{G}_A^0$ is closely related to the class of Hyperbolic distributions (see Frery et al., 1995). Figure 3 shows the densities of the $\mathcal{G}_A^0$ and Gaussian distributions, with parameters $(-3, 1, 1)$ and $(3\pi/16, 1/2 - 9\pi^2/256)$, respectively, in semilogarithmic scale. Such parameters were

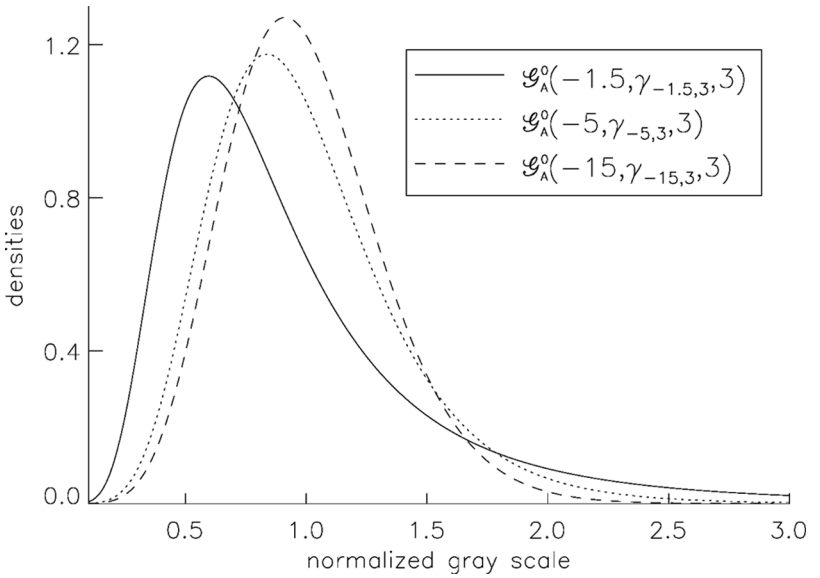

Figure 2. Densities of the $\mathcal{G}_A^0(\alpha, \gamma_{\alpha,3}, 3)$ distribution.

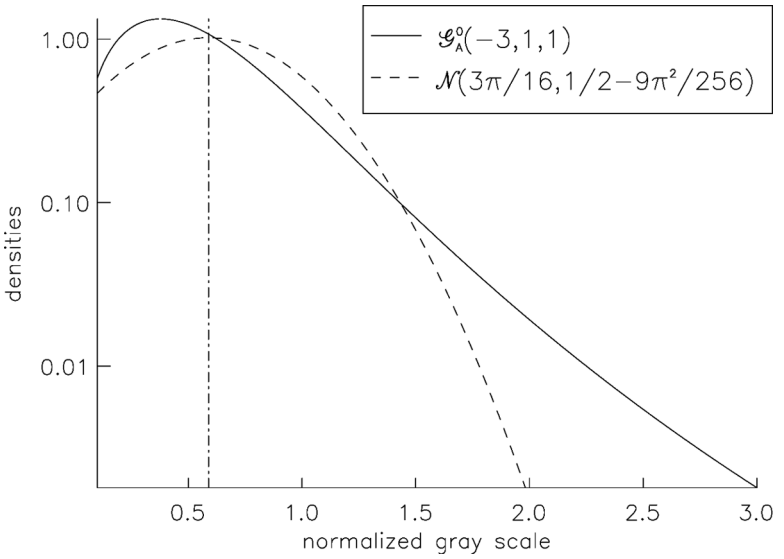

Figure 3. Densities of the $\mathcal{G}_A^0$ and Gaussian distributions with same mean values $\mu = 3\pi/16$ in semilogarithmic scale.

chosen distributions so that these distributions have equal mean (shown as the vertical line at $\mu = 3\pi/16$) and variance. The different decay of the tails is evident: the former behaves as a logarithm, while the latter decays in quadratic fashion. This behavior ensures the ability of the $\mathcal{G}_A^0$ distribution to model data with extreme variability.

Besides being essential for the simulation technique here proposed, cumulative distribution functions are needed for carrying out goodness of fit tests and for the proposal of estimators based on order statistics. It can be seen in Mejail et al. (2000, 2003) that the cumulative distribution function of a $\mathcal{G}_A^0(\alpha, \gamma, n)$ distributed random variable is given, for every $z > 0$, by $G(z, (\alpha, \gamma, n)) = \Upsilon_{2n,-2\alpha}(-\alpha z^2/\gamma)$, where $\Upsilon_{s,t}$ is the cumulative distribution function of a Snedecor's $F_{s,t}$ distributed random variable with s and t degrees of freedom. Both $\Upsilon_{\cdot,\cdot}$ and $\Upsilon_{\cdot,\cdot}^{-1}$ are readily available in most platforms for computational statistics.

The single look case is of particular interest since it describes the noisiest images and it exhibits nice analytical properties. The distribution is characterized by the density

$$f(z; \alpha, \gamma, 1) = -\frac{2\alpha}{\gamma^\alpha} z(\gamma + z^2)^{\alpha-1} \mathbb{I}_{0,\infty}(z), \quad -\alpha, \gamma > 0.$$

Its cumulative distribution function is given by $F(t) = (1 - (1 + t^2/\gamma)^\alpha)\mathbb{I}_{(0,\infty)}(t)$, and its inverse, useful for the generation of random deviates and the computation of quantiles, is given by $F^{-1}(t) = (\gamma((1-t)^{\frac{1}{\alpha}} - 1))^{\frac{1}{2}} \mathbb{I}_{(0,1)}(t)$.

2.2. *Correlated Clutter*

Instead of defining the model over $\mathbb{Z}^2$, a realistic description of finite-sized fields is made in this section. Let $Z_A = (Z_A(k, \ell))_{0 \le k \le N-1, 0 \le \ell \le N-1}$ be the stochastic model that describes the return amplitude image.

Definition 2.1. We say that Z_A is a $\mathcal{G}_A^0(\alpha, \gamma, n)$ stochastic process with correlation function ρ_{Z_A} (in symbols $Z_A \sim (\mathcal{G}_A^0(\alpha, \gamma, n), \rho_{Z_A})$) if for all $0 \leq i, j, k, \ell \leq N-1$ holds that

1. $Z_A(k, \ell)$ obeys a $\mathcal{G}_A^0(\alpha, \gamma, n)$ law;
2. the mean field is $\mu_{Z_A} = E(Z_A(k, \ell))$;
3. the variance field is $\sigma^2_{Z_A} = \mathrm{Var}(Z_A(k, \ell))$;
4. the correlation function is $\rho_{Z_A}((i, j), (k, \ell)) = (E(Z_A(i, j)Z_A(k, \ell)) - \mu^2_{Z_A})/\sigma^2_{Z_A}$.

The scale property of the parameter γ implies that correlation function ρ_{Z_A} and γ are unrelated and, therefore, it is enough to generate a $Z_A^1 \sim (\mathcal{G}_A^0(\alpha, \gamma, n), \rho_{Z_A})$ field and then simply multiply every outcome by $\gamma^{1/2}$ to get the desired field.

This article presents a variation of a method used for simulation of correlated Gamma variables, called Transformation Method, that can be found in Bustos et al. (2001a,b). This method can be summarized in the following three steps.

1. Generate independent outcomes from a convenient distribution.
2. Introduce correlation in these data.
3. Transform the correlated observations into data with the desired marginal properties.

The transformation that guarantees the validity of this procedure is obtained from the cumulative distribution functions of the data obtained in step 2, and from the desired set of distributions.

Recall that if U is a continuous random variable with cumulative distribution function F_U then $F_U(U)$ obeys a uniform $\mathcal{U}(0, 1)$ law and, reciprocally, if V obeys a $\mathcal{U}(0, 1)$ distribution then $F_U^{-1}(V)$ is F_U distributed. In order to use this method it is necessary to know the correlation that the random variables will have after the transformation, besides the function F_U^{-1}.

The method here studied consists of the following steps.

1. Propose a correlation structure for the $\mathcal{G}_A^0$ field, say, the function ρ_{Z_A}.
2. Generate a field of independent identically distributed standard Gaussian observations.
3. Compute τ, the correlation structure to be imposed to the Gaussian field from ρ_{Z_A}, and impair it using the Fourier transform without altering the marginal properties.
4. Transform the correlated Gaussian field into a field of observations of identically distributed $\mathcal{U}(0, 1)$ random variables, using the cumulative distribution function of the Gaussian distribution (Φ).
5. Transform the uniform observations into $\mathcal{G}_A^0$ outcomes, using the inverse of the cumulative distribution function of the $\mathcal{G}_A^0$ distribution (G^{-1}).

The function that relates ρ_{Z_A} and τ is computed using numerical tools. In principle, there are no restrictions on the possible roughness parameters values that can be obtained by this method, but issues related to machine precision must be taken into account. Another important issue is that not every desired final correlation structure ρ_{Z_A} is mapped onto a feasible intermediate correlation structure τ. The procedure is presented in detail in the next section.

3. Transformation Method

Let $G(\cdot, (\alpha, \gamma, n))$ be the cumulative distribution function of a $\mathcal{G}_A^0(\alpha, \gamma, n)$ distributed random variable. As previously stated,

$$G(x, (\alpha, \gamma, n)) = \Upsilon_{2n,-2\alpha}\left(-\frac{\alpha x^2}{\gamma}\right),$$

where Υ_{v_1,v_2} is the cumulative distribution function of a Snedecor F_{v_1,v_2} distribution, i.e.,

$$\Upsilon_{v_1,v_2}(x) = \frac{\Gamma\left(\frac{v_1+v_2}{2}\right)}{\Gamma\left(\frac{v_1}{2}\right)\Gamma\left(\frac{v_2}{2}\right)}\left(\frac{v_1}{v_2}\right)^{\frac{v_1}{2}}\int_0^x t^{\frac{v_1-2}{2}}\left(1+\frac{v_1}{v_2}t\right)^{-\frac{v_1+v_2}{2}} dt.$$

The inverse of $G(\cdot, (\alpha, \gamma, n))$ is, therefore

$$G^{-1}(t, (\alpha, \gamma, n)) = \sqrt{-\frac{\gamma}{\alpha}\Upsilon_{2n,-2\alpha}^{-1}(t)}.$$

To generate $Z_A^1 = (Z_A^1(k, \ell))_{0\le k\le N-1, 0\le \ell\le N-1} \sim (\mathcal{G}_A^0(\alpha, 1, n), \rho_{Z_A})$ using the inversion method we define every coordinate of the process Z_A as a transformation of a Gaussian process ζ as $Z_A^1(i, j) = G^{-1}(\Phi(\zeta(i, j)), (\alpha, 1, n))$, where $\zeta = (\zeta(i, j))_{0\le i\le N-1, 0\le j\le N-1}$ is a stochastic process such that $\zeta(i, j)$ is a standard Gaussian random variable and with correlation function τ_ζ (i.e., where $\tau_\zeta((i, j), (k, \ell)) = E(\zeta(i, j)\zeta(k, \ell))$) satisfying

$$\rho_{Z_A}((i, j), (k, \ell)) = \varrho_{(\alpha,n)}(\tau_\zeta((i, j), (k, \ell))) \tag{3}$$

for all $0 \le i, j, k, \ell \le N-1$ and $(i, j) \ne (k, \ell)$ and where Φ denotes the cumulative distribution function of a standard Gaussian random variable and the function $\varrho_{(\alpha,n)}$ will be defined below in Eq. (4).

Posed as a diagram, the method consists of the following transformations among Gaussian ($\mathcal{N}$), Uniform ($\mathcal{U}$), and $\mathcal{G}_A^0$-distributed random variables:

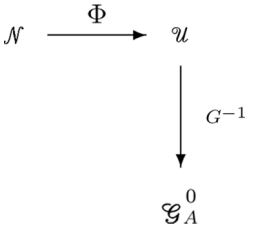

A central issue of the method is finding the correlation structure that the Gaussian field has to obey, in order to have the desired $\mathcal{G}_A^0$ field after the transformation. The function $\varrho_{(\alpha,n)}$ is defined on $(-1, 1)$ by

$$\varrho_{(\alpha,n)}(\tau) = \frac{R_{(\alpha,n)}(\tau) - \left(\frac{1}{n}\right)\left(\frac{\Gamma(n+\frac{1}{2})\Gamma(-\alpha-\frac{1}{2})}{\Gamma(n)\Gamma(-\alpha)}\right)^2}{-\frac{1}{1+\alpha} - \left(\frac{1}{n}\right)\left(\frac{\Gamma(n+\frac{1}{2})\Gamma(-\alpha-\frac{1}{2})}{\Gamma(n)\Gamma(-\alpha)}\right)^2}, \tag{4}$$

with

$$R_{(\alpha,n)}(\tau) = \int\int_{\mathbb{R}^2} G^{-1}(\Phi(u), (\alpha, 1, n))G^{-1}(\Phi(v), (\alpha, 1, n))\phi_2(u, v, \tau)du\,dv$$

where

$$\phi_2(u, v, \tau) = \frac{1}{2\pi\sqrt{(1-\tau^2)}} \exp\left(-\frac{u^2 - 2\tau \cdot u \cdot v + v^2}{2(1-\tau^2)}\right).$$

Note that $R_{(\alpha,n)}(\tau_\zeta((i, j), (k, \ell))) = E(Z_A^1(i, j)Z_A^1(k, \ell))$ for all $0 \le i, j, k, \ell \le N-1$ and $(i, j) \ne (k, \ell)$.

The answer to the question of finding τ_ζ given ρ_{Z_A} is equivalent to the problem of inverting the function $\varrho_{(\alpha,n)}$. This function is available using numerical methods.

3.1. *Inversion of $\varrho_{(\alpha,n)}$*

The function $\varrho_{(\alpha,n)}$ has the following properties.

1. The set $\{\varrho_{(\alpha,n)}(\tau) : \tau \in (-1, 1)\}$ is strictly included in $(-1, 1)$, and depends on the values of α.
2. The function $\varrho_{(\alpha,n)}$ is strictly increasing in $(-1, 1)$.
3. The values $\varrho_{(\alpha,n)}(\tau)$ are strictly negative for all $\tau < 0$.

Let $\eth_{(\alpha,n)}$ be the inverse function of $\varrho_{(\alpha,n)}$. Then, in order to calculate its value for a fixed $\rho \in (-1, 1)$, we have to solve the following equation in τ:

$$R_{(\alpha,n)}(\tau) + \frac{\rho}{1+\alpha} + (\rho - 1)\left(\frac{1}{n}\right)\left(\frac{\Gamma(n + \frac{1}{2}\Gamma(-\alpha - \frac{1}{2})}{\Gamma(n)\Gamma(-\alpha)}\right)^2 = 0.$$

Then, it follows from the properties of $\varrho_{(\alpha,n)}$, that for certain values of α the set of τ such that this equation is solvable is a strict subset of $(-1, 1)$. Table 1 shows some values of the function $\eth_{(\alpha,n)}$ for specific values of ρ, n, and α. Figure 4 shows τ as a function of ρ for the $n = 1$ case and varying values of α, and it can be seen that the smaller α the closer this function is to the identity. This is sensible, since the $\mathcal{G}_A^0$ distribution becomes more and more symmetric as $\alpha \to -\infty$ and, therefore, simulating outcomes from this distribution becomes closer and closer to the problem of obtaining Gaussian deviates.

Figure 5 presents the same function for $\alpha = -1.5$ and varying number of looks. It is noticeable that τ is far less sensitive to n than to α, a feature that suggests a shortcut for computing the values of Table 1: disregarding the dependence on n, i.e., considering $\tau(\rho, \alpha, n) \simeq \tau(\rho, \alpha, n_0)$ for a fixed convenient n_0.

The source FORTRAN file with routines for computing the functions $\varrho_{(\alpha,n)}$ and $\eth_{(\alpha,n)}$ can be obtained from the first author of this article.

3.2. *Generation of the Process ζ*

The process ζ, that consists of spatially correlated standard Gaussian random variables, will be generated using a spectral technique that employs the Fourier transform. This method has computational advantages with respect to the direct application of a convolution filter. Again, the concern here is to define a finite process instead of working on $\mathbb{Z}^2$ for the sake of simplicity.

Table 1
Values of $\delta_{(\alpha,n)}$

	$\alpha = -1.5$				$\alpha = -3.0$				$\alpha = -9.0$			
ρ	$n = 1$	$n = 3$	$n = 6$	$n = 10$	$n = 1$	$n = 3$	$n = 6$	$n = 10$	$n = 1$	$n = 3$	$n = 6$	$n = 10$
−.9										−.953	−.954	−.958
−.8									−.877	−.845	−.845	−.848
−.7					−.886	−.881	−.901	−.915	−.763	−.737	−.737	−.740
−.6					−.747	−.745	−.761	−.772	−.650	−.630	−.630	−.632
−.5					−.613	−.612	−.624	−.632	−.539	−.523	−.523	−.525
−.4	−.844	−.903	−.948	−.972	−.483	−.483	−.492	−.498	−.429	−.417	−.417	−.419
−.3	−.591	−.630	−.656	−.670	−.357	−.357	−.363	−.367	−.320	−.312	−.312	−.313
−.2	−.370	−.392	−.405	−.412	−.234	−.235	−.239	−.241	−.212	−.207	−.207	−.208
−.1	−.174	−.183	−.188	−.190	−.116	−.116	−.117	−.119	−.105	−.103	−.103	−.104
0	.0	.0	.0	.0	.0	.0	.0	.0	.0	.0	.0	.0
.1	.155	.161	.164	.165	.112	.113	.114	.115	.104	.103	.103	.103
.2	.294	.303	.307	.309	.222	.223	.225	.226	.208	.205	.205	.205
.3	.418	.428	.433	.435	.328	.329	.332	.334	.310	.306	.306	.307
.4	.529	.539	.544	.546	.432	.433	.436	.438	.411	.407	.407	.408
.5	.629	.638	.642	.644	.533	.534	.537	.539	.512	.507	.508	.508
.6	.719	.727	.730	.731	.631	.633	.635	.637	.611	.607	.607	.608
.7	.800	.806	.808	.809	.727	.728	.731	.732	.710	.706	.706	.707
.8	.873	.877	.879	.880	.820	.821	.823	.824	.807	.805	.805	.805
.9	.940	.942	.942	.943	.911	.912	.913	.913	.904	.903	.903	.903

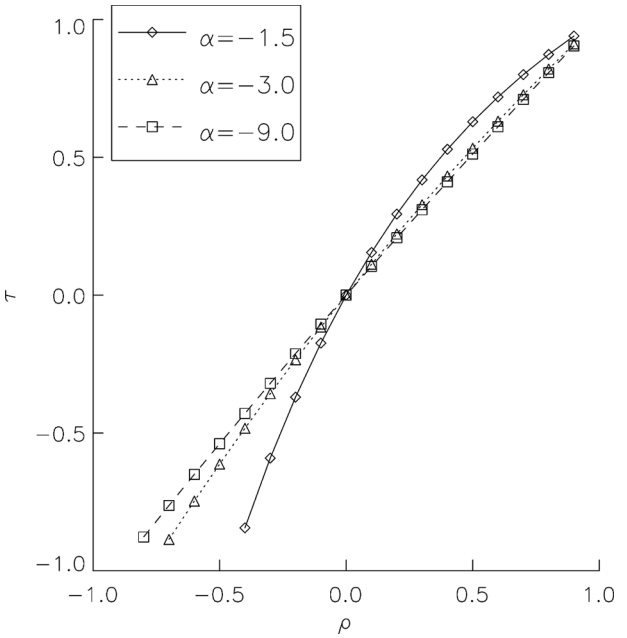

Figure 4. Values of τ as a function of ρ for $n = 1$ and varying α.

We should notice that the usual simulation method of such Gaussian vectors is based on inverting their correlation matrix, and it is not computationally feasible in the case of remote sensing imagery. In this case, it would involve the computation of the inverse of a huge matrix. Even for the case of a very small image, let say 32×32 pixels, we should invert a matrix of dimension $(32 \times 32)(32 \times 32)$. For remote sensing images, the general size is about $3{,}000 \times 3{,}000$ pixels.

Consider the following sets:

$$
\begin{aligned}
R_1 &= \{(k, \ell) : 0 \le k, \ell \le N/2\},\\
R_2 &= \{(k, \ell) : N/2 + 1 \le k \le N - 1, 0 \le \ell \le N/2\},\\
R_3 &= \{(k, \ell) : 0 \le k \le N/2, N/2 + 1 \le \ell \le N - 1\},\\
R_4 &= \{(k, \ell) : N/2 + 1 \le k \le N - 1, N/2 + 1 \le \ell \le N - 1\},\\
R_N &= R_1 \cup R_2 \cup R_3 \cup R_4 = \{(k, \ell) : 0 \le k, \ell \le N - 1\},\\
\overline{R_N} &= \{(k, \ell) : -\{N - 1) \le k, \ell \le N - 1\}.
\end{aligned}
$$

Let $\rho : R_1 \longrightarrow (-1, 1)$ be a function, extended onto $\overline{R_N}$ by:

$$
\rho(k, \ell) = \begin{cases}
\rho(N - k, \ell) & \text{if } (k, \ell) \in R_2,\\
\rho(k, N - \ell) & \text{if } (k, \ell) \in R_3,\\
\rho(N - k, N - \ell) & \text{if } (k, \ell) \in R_4,\\
\rho(N + k, \ell) & \text{if } -(N - 1) \le k < 0 \le \ell \le N - 1,\\
\rho(k, N + \ell) & \text{if } -(N - 1) \le \ell < 0 \le k \le N - 1,\\
\rho(N + k, N + \ell) & \text{if } -(N - 1) \le k, \ \ \ell < 0.
\end{cases}
$$

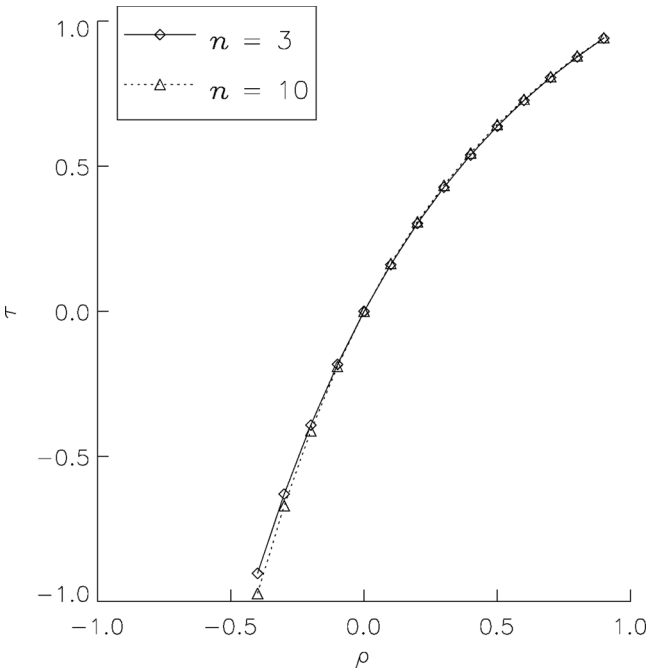

Figure 5. Values of τ as a function of ρ for $\alpha = -1.5$ and varying n.

Let $Z_A = (Z_A(k, \ell))_{0 \le k \le N-1, 0 \le \ell \le N-1}$ be a $\mathcal{G}_A^0(\alpha, \gamma, n)$ stochastic process with correlation function ρ_{Z_A} defined by $\rho_{Z_A}((k_1, \ell_1), (k_2, \ell_2)) = \rho(k_2 - k_1, \ell_2 - \ell_1)$. Assume that $\tau(k, \ell) = \eth_{(\alpha,n)}(\rho(k, \ell))$ is defined for all (k, ℓ) in R_N.

Let $\mathcal{F}(\tau) : R_N \longrightarrow \mathbb{C}$ be the normalized Fourier Transform of τ, that is,

$$\mathcal{F}(\tau)(k, \ell) = \frac{1}{N^2} \sum_{k_1=0}^{N-1} \sum_{\ell_1=0}^{N-1} \tau(k_1, \ell_1) \exp(-2\pi i(k \cdot k_1 + \ell \cdot \ell_1)/N^2).$$

Let $\psi : R_N \longrightarrow \mathbb{C}$ be defined by $\psi(k, \ell) = \sqrt{\mathcal{F}(\tau)(k, \ell)}$ and let the function $\theta : \overline{R_N} = \{(k, \ell) : -(N-1) \le k, \ell \le N-1\} \longrightarrow \mathbb{R}$ be defined by

$$\theta(k, \ell) = \mathcal{F}^{-1}(\psi)(k, \ell)/N = \frac{1}{N} \sum_{k_1=0}^{N-1} \sum_{\ell_1=0}^{N-1} \psi(k_1, \ell_1) \exp(-2\pi i(k \cdot k_1 + \ell \cdot \ell_1)/N^2)$$

(the normalized inverse Fourier Transform of ψ) for all $(k, \ell) \in R_N$; and

$$\theta(k, \ell) = \begin{cases} \theta(N + k, \ell) & \text{if } -(N-1) \le k < 0 \le \ell \le N-1, \\ \theta(k, N + \ell) & \text{if } -(N-1) \le \ell < 0 \le k \le N-1, \\ \theta(N + k, N + \ell) & \text{if } -(N-1) \le k, \ \ell < 0. \end{cases}$$

A straightforward calculation shows that

$$(\theta * \theta)(k, \ell) = \sum_{k_1=0}^{N-1} \sum_{\ell_1=0}^{N-1} \theta(k_1, \ell_1)\theta(k - k_1, \ell - \ell_1) = \tau(k, \ell),$$

for all $(k, \ell) \in R_N$.

Remark 3.1. The fact that $\mathcal{F}(\tau)(k, \ell) \geq 0$ and the last equality for all $(k, \ell) \in R_N$ is easily deduced from the results in Sec. 5.5 of Jain (1989); more details can be seen in Kay (1988).

Finally, we define $\zeta = (\zeta(i, j))_{0 \leq i \leq N-1, 0 \leq j \leq N-1}$ by

$$\zeta(k, \ell) = (\theta * \xi)(k, \ell) = N\mathcal{F}^{-1}((\psi\mathcal{F}(\xi)))(k, \ell),$$

where $\xi = (\xi(k, \ell))_{(k,\ell) \cdot \in R_N}$ is a Gaussian white noise with standard deviation 1.

Then it is easy to prove that $\zeta = (\zeta(i, j))_{0 \leq i \leq N-1, 0 \leq j \leq N-1}$ is a stochastic process such that $\zeta(i, j)$ is a standard Gaussian random variable with correlation function τ_ζ satisfying Eq. (3).

3.3. *Implementation*

The results presented in previous sections were implemented using the IDL version 7.1 development platform, with the following algorithm.

Algorithm 3.1. Input: $\alpha < -1, \gamma > 0, n \geq 1$ integer, ρ and τ functions as above, then:

1. Compute the frequency domain mask $\psi(k, \ell) = \sqrt{\mathcal{F}(\tau)(k, \ell)}$.
2. Generate $\xi = (\xi(k, \ell))_{(k,\ell) \in R_N}$, the Gaussian white noise with zero mean and variance 1.
3. Calculate $\zeta(k, \ell) = N\mathcal{F}^{-1}((\psi \cdot \mathcal{F}(\xi)))(k, \ell)$, for every (k, ℓ).
4. Obtain $Z_A^1(k, \ell) = G^{-1}(\Phi(\zeta(k, \ell)), (\alpha, 1, n))$, for every (k, ℓ).
5. Return $Z_A(k, \ell) = \sqrt{\gamma} Z_A^1(k, \ell)$ for every (k, ℓ).

4. Simulation Results

In practice, both parametric and nonparametric correlation structures are of interest. The former relies on analytic forms for ρ, while the latter merely specifies values for the correlation. Parametric forms for the correlation structure are simpler to specify, and its inference amounts to estimating a few numerical values; nonparametric forms do not suffer from lack of adequacy, but demand the specification (and possibly the estimation) of potentially large sets of parameters.

In the following examples, the technique presented above will be used to generate samples from both parametric and nonparametric correlation structures.

Example 4.1 (Parametric Model)**.** This correlation model is very popular in applications. Consider $L \geq 2$ an even integer, $0 < a < 1, \varepsilon > 0$ (for example $\varepsilon = 0.001$), $\alpha < -1$ and $n \geq 1$. Let $h : \mathbb{R} \longrightarrow R$ be defined by

$$h(x) = \begin{cases} x & \text{if } |x| \geq \varepsilon, \\ 0 & \text{if } |x| < \varepsilon. \end{cases}$$

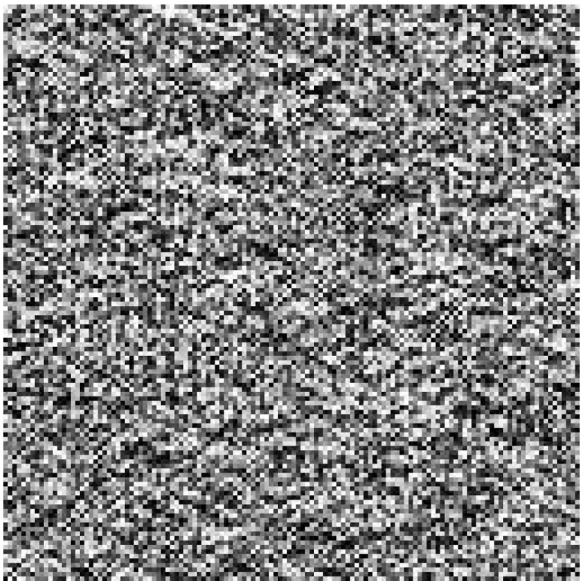

Figure 6. Correlated $\mathcal{G}^0(-1.5, 1, 1)$-distributed amplitude image with the correlation structure defined in Example 4.1.

Let $\rho : R_x \longrightarrow (-1, 1)$ be defined by $\rho(0, 0) = 1$, and if $(k, \ell) \neq (0, 0)$ in R_1 by:

$$\rho(k, \ell) = \begin{cases} h(a \exp(-k^2/L^2)) & \text{if } k \geq \ell, \\ -h(a \exp(-\ell^2/L^2)) & \text{if } k < \ell. \end{cases}$$

The image shown in Fig. 6, of size 128×128, was obtained assuming $a = 0.4$, $L = 2$, $\alpha = -1.5$, $\gamma = 1.0$, and $n = 1$.

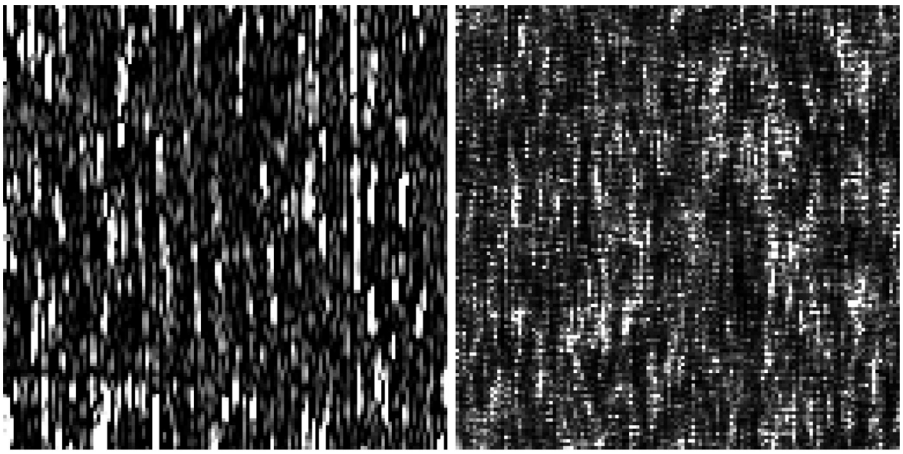

(a) (b)

Figure 7. Real urban area and simulated data: (a) Urban area and (b) Correlated clutter.

Example 4.2 (Nonparametric Specification)**.** The starting point is the urban area shown in Fig. 7(a). This 128×128 pixels image is a small sample of data obtained by the E-SAR system over an urban area. The complete dataset was used as input for estimating the correlation structure defined by an 16×16 correlation matrix using Pearson's procedure ($\hat{\rho}$ below, where only values larger than 10^{-3} are shown; see Appendix A). The correlation structure for the Gaussian process is τ below, where only values larger than 10^{-3} are shown. The roughness and scale parameters were estimated using the moments technique. The simulated $\mathcal{G}_A^0$ field is shown in Fig. 7(b).

$$\hat{\rho} = \begin{pmatrix} 1.00 & 0.65 & 0.22 \\ 0.97 & 0.63 & 0.22 \\ 0.88 & 0.58 & 0.21 \\ 0.76 & 0.50 & 0.19 \\ 0.64 & 0.43 & 0.16 \\ 0.53 & 0.36 & 0.14 \\ 0.43 & 0.30 & 0.12 \\ 0.36 & 0.25 & 0.10 \\ 0.29 & 0.20 & 0.00 \\ 0.24 & 0.17 & 0.00 \\ 0.20 & 0.13 & 0.00 \\ 0.16 & 0.11 & 0.00 \\ 0.13 & 0.00 & 0.00 \\ 0.11 & 0.00 & 0.00 \end{pmatrix}, \quad \tau = \begin{pmatrix} 1.00 & 0.76 & 0.32 \\ 0.98 & 0.74 & 0.32 \\ 0.93 & 0.70 & 0.31 \\ 0.85 & 0.63 & 0.28 \\ 0.75 & 0.56 & 0.24 \\ 0.68 & 0.49 & 0.21 \\ 0.56 & 0.42 & 0.18 \\ 0.49 & 0.36 & 0.16 \\ 0.41 & 0.294 & 0.00 \\ 0.35 & 0.25 & 0.00 \\ 0.29 & 0.20 & 0.00 \\ 0.24 & 0.17 & 0.00 \\ 0.20 & 0.00 & 0.00 \\ 0.17 & 0.00 & 0.00 \end{pmatrix}$$

Example 4.3 (Mosaic)**.** A mosaic of nine simulated fields is shown in Fig. 8(a). Each field is of size 128×128 and obeys the model presented in Example 4.1 with $a = 0.4$, $\gamma = 1.0$, $n = 1$, roughness a varying m the rows (-1.5, -3.0, and -9.0 from top to bottom) and correlation length L varying along the columns (2, 4, and 8 from left to right). The popularity of this correlation structure is partly due to the appealing results, when compared with real imagery from deforested or pasture areas, forest on flat relief and primary forest on undulated relief shown in Fig. 8(b). Notice the shadowing effect of the last sample, and how different it is from the one observed on Fig. 7(b), which corresponds to urban area.

5. Conclusions and Future Work

A method for the simulation of correlated clutter with desirable marginal law and correlation structure was presented. This method allows the obtainment of precise and controlled first and second-order statistics, and can be easily implemented using standard numerical tools. The technique is quite general, and allows the specification of both parametric and nonparametric correlation structures.

The adequacy of the method for the simulation of several scenarios was assessed using real data, as presented in Example 4.2: estimating the underlying correlation structure of an urban area and then simulating fields with it. We have also shown a mosaic of nine simulated fields, computed using a parametric correlation structure

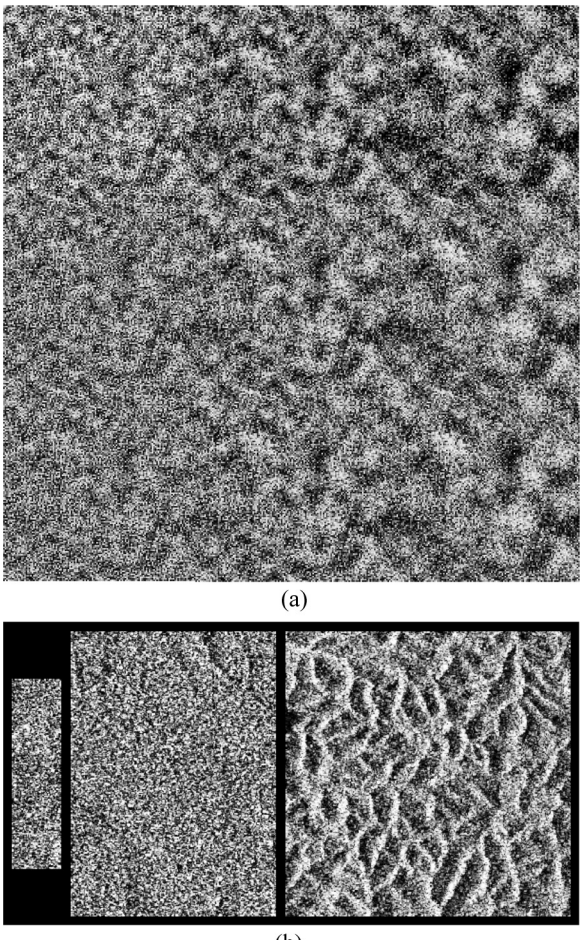

(a)

(b)

Figure 8. Real samples from JERS-1 data and simulated correlated return: (a) Mosaic of nine simulated fields and (b) Real data: pasture, forest on flat relief and primary forest on undulated relief.

that mimics the characteristic shadowing of primary forest on undulated relief. Urban areas and forest areas are both heavy correlated, but their correlation structures are very different. Our simulation method allows us to mimic these differences, making its output suitable for testing classification schemes.

We can summarize the trend of our future research as follows:

1. Extension of current methodology to multidimensional SAR models, generated by different sources like baseline, polarization, frequency, time as well as their different combinations;
2. Utilization of more sophisticated models being able to take into consideration all available a priori information and knowledge;
3. Utilization of an integrated platform with high numerical performance.

Bustos and Frery (2005) showed that IDL may present numerical instabilities, while Almiron et al. (in press) conducted an analysis of platforms showing that

R (freely available at http://www.r-project.org) has excellent numerical performance. The authors are migrating the implementation from the former to the latter platform avoiding, also, the use of FORTRAN code.

Appendix A: Estimating Correlation Structure with Pearson's Method

Consider the image $\mathbf{z}$ with M rows and N columns

$$\mathbf{z} = \begin{bmatrix} z(0,0) & \cdots & z(N-1,0) \\ \vdots & \ddots & \vdots \\ z(0,M-1) & \cdots & z(N-1,M-1) \end{bmatrix}$$

and n_v a positive integer smaller than $\min(M,N)$. Define $n_c = [N/(2n_v)]$ and $n_f = [M/(2n_v)]$, where $[x] = \max\{k \in \mathbb{N} : k \le x\}$ for every real number x. For each $i = 0, \ldots, n_c - 1$ and each $j = 0, \ldots, n_f - 1$ define $\mathbf{c}(i,j)$ the submatrix of $\mathbf{z}$ of size $2n_v \times 2n_v$ given by

$$\mathbf{c}(i,j) = \begin{bmatrix} z(2n_v i, 2n_v j) & \cdots & z(2n_v i + 2n_v - 1, 2n_v j) \\ \vdots & \ddots & \vdots \\ z(2n_v i, 2n_v j + 2n_v - 1) & \cdots & z(2n_v i + 2n_v - 1, 2n_v j + 2n_v - 1) \end{bmatrix},$$

and let $\mathbf{z}_v(i,j)$ be the submatrix of $\mathbf{c}(i,j)$ of size $n_v \times n_v$ given by

$$\mathbf{z}_v(i,j) = \begin{bmatrix} z(2n_v i, 2n_v j) & \cdots & z(2n_v i + n_v - 1, 2n_v j) \\ \vdots & \ddots & \vdots \\ z(2n_v i, 2n_v j + n_v - 1) & \cdots & z(2n_v i + n_v - 1, 2n_v j + n_v - 1) \end{bmatrix}.$$

We will consider that $\mathbf{z}_v(i,j)$, for every $i = 0, \ldots, n_c - 1$ and every $j = 0, \ldots, n_f - 1$, is a sample of the random matrix

$$\mathbf{Z} = \begin{bmatrix} Z(0,0) & \cdots & Z(n_v - 1, 0) \\ \vdots & \ddots & \vdots \\ Z(0, n_v - 1) & \cdots & Z(n_v - 1, n_v - 1) \end{bmatrix}.$$

The autocorrelation function of the random matrix $\mathbf{Z}$ is defined as

$$\rho_{\mathbf{z}}((m,n),(k,\ell)) = \frac{E(Z(m,n)Z(k,\ell)) - \mu_z(m,n)\mu_z(k,\ell)}{\sigma_z(m,n)\sigma_z(k,\ell)},$$

where $\mu_z(k,\ell) = E(Z(k,\ell))$ and $\sigma_z(k,\ell) = \sqrt{\mathrm{Var}(Z(k,\ell))}$, for every $0 \le m, n, k, \ell \le n_v - 1$.

The function $\rho_{\mathbf{z}}$ can be estimated using Pearson's sample correlation coefficient based on $\mathbf{z}_v(i,j), i = 0, \ldots, n_c - 1$ and $j = 0, \ldots, n_f - 1$, i.e., for $0 \le m, n, k, \ell \le n_v - 1$ by

$$r_{\mathbf{z}}((m,n),(k,\ell)) = \frac{C_{\mathbf{z}}((m,n),(k,\ell))}{s_{\mathbf{z}}(m,n)s_{\mathbf{z}}(k,\ell)},$$

where

$$C_{\mathbf{z}}((m,n),(k,\ell)) = \sum_{j=0}^{n_f-1}\sum_{i=0}^{n_c-1}(z(2n_v i+m, 2n_v j+n) - \bar{z}(m,n)) \times (z(2n_v i+k, 2n_v j+\ell) - \bar{z}(k,\ell)),$$

$$s_{\mathbf{z}}(m,n) = \sqrt{\sum_{j=0}^{n_f-1}\sum_{i=0}^{n_c-1}(z(2n_v i+m, 2n_v j+n) - \bar{z}(m,n))^2},$$

$$\bar{z}(m,n) = \frac{1}{n_c n_f}\sum_{j=0}^{n_f-1}\sum_{i=0}^{n_c-1} z(2n_v i+m, 2n_v j+n).$$

Acknowledgments

This work was partially supported by Conicet and SeCyT grants 69/08, 05/B352 (Argentina) and CNPq (Brazil).

References

Allende, H., Frery, A. C., Galbiati, J., Pizarro, L. (2006). *M*-estimators with asymmetric influence functions: The GA0 distribution case. *Journal of Statistical Computation and Simulation* 76:941–956.

Almiron, M., Almeida, E. S., Miranda, M. (in press). The reliability of statistical functions in four software packages freely used in numerical computation. *Brazilian Journal of Probability and Statistics*.

Barndorff-Nielsen, O. E., Blæsild, P. (1981). Hyperbolic distributions and ramifications: Contributions to theory and applications. In: Taillie, C., Baldessari, B. A., eds. *Statistical Distributions in Scientific Work*. Dordrecht: Reidel, pp. 19–44.

Bustos, O. H., Flesia, A. G., Frery, A. C. (2001a). Generalized method for sampling spatially correlated heterogeneous speckled imagery. *EURASIP Journal on Applied Signal Processing* 89–99.

Bustos, O. H., Flesia, A. G., Frery, A. C. (2001b). Performance of spectral estimators in simulated synthetic aperture radar images. *Latin American Applied Research* 31:93–98.

Bustos, O. H., Frery, A. C. (2005). Statistical functions and procedures in IDL 5.6 and 6.0. *Computational Statistics and Data Analysis* 50:301–310.

Bustos, O. H., Lucini, M. M., Frery, A. C. (2002). *M*-estimators of roughness and scale for GA0-modelled SAR imagery. *EURASIP Journal on Applied Signal Processing* (1):105–114.

Cribari-Neto, F., Frery, A. C., Silva, M. F. (2002). Improved estimation of clutter properties in speckled imagery. *Computational Statistics and Data Analysis* 40(4):801–824.

Frery, A. C., Yanasse, C. C. F., Sant'Anna, S. J. S. (1995). Alternative distributions for the multiplicative model in SAR images. In: *International Geoscience and Remote Sensing Symposium: Quantitative Remote Rensing for Science and Applications*. Florence, July, IEEE Computer Society, IGARSS'95 Proc., pp. 169–171.

Frery, A. C., Müller, H.-J., Yanasse, C. C. F., Sant'Anna, S. J. S. (1997). A model for extremely heterogeneous clutter. *IEEE Transactions on Geoscience and Remote Sensing* 35(3):648–659.

Frery, A. C., Correia, A. H., Renn'o, C. D., Freitas, C. C., Jacobo-Berlles, J., Mejail, M. E., Vasconcellos, K. L. P. (1999). Models for synthetic aperture radar image analysis. *Resenhas (IME-USP)* 4(1):45–77.

Frery, A. C., Cribari-Neto, F., Souza, M. O. (2004). Analysis of minute features in speckled imagery with maximum likelihood estimation. *EURASIP Journal on Applied Signal Processing* 16:2476–2491.

Gambini, J., Mejail, M., Jacobo-Berlles, J., Frery, A. C. (2006). Feature extraction in speckled imagery using dynamic B-spline deformable contours under the G0 model. *International Journal of Remote Sensing* 27:5037–5059.

IDL 7.1 Language. ITT Visual Information Solutions.

Jain, A. K. (1989). *Fundamentals of Digital Image Processing*. Englewood Cliffs, NJ: Prentice-Hall International Editions.

Kay, S. M. (1988). *Modern Spectral Estimation: Theory & Application*. Englewood Cliffs, NJ: Prentice Hall.

Mejail, M. E., Frery, A. C., Jacobo-Berlles, J., Bustos, O. H. (2000). Parametric roughness estimation in amplitude SAR images under the multiplicative model. *Revista de Teledetección* 13:37–49.

Mejail, M. E., Frery, A. C., Jacobo-Berlles, J., Bustos, O. H. (2001). Approximation of distributions for SAR images: proposal, evaluation and practical consequences. *Latin American Applied Research* 31:83–92.

Mejail, M. E., Jacobo-Berlles, J., Frery, A. C., Bustos O. H. (2003). Classification of SAR images using a general and tractable multiplicative model. *International Journal of Remote Sensing* 24(18):3565–3582.

Moschetti, E., Palacio, M. G., Picco, M., Bustos, O. H., Frery, A. C. (2006). On the use of Lee's protocol for speckle-reducing techniques. *Latin American Applied Research* 36(2):115–121.

Nascimento, A. D. C., Cintra, R. J., Frery, A. C. (in press). Hypothesis testing in speckled data with stochastic distances. *IEEE Transactions on Geoscience and Remote Sensing*.

Silva, M., Cribari-Neto, F., Frery, A. C. (2008). Improved likelihood inference for the roughness parameter of the GA0 distribution. *Environmetrics* 19:347–368.

Vasconcellos, K. L. P., Frery, A. C., Silva, L. B. (2005). Improving estimation in speckled imagery. *Computational Statistics* 20:503–519.